Operator State in a Workplace Simulation Modulates Eye-Blink Related EEG Activity

Emad Alyan, Edmund Wascher, Stefan Arnau, Ruth Kaesemann, and Julian Elias Reiser

***Abstract*— Evaluating and understanding the cognitive demands of natural activities has been difficult using neurocognitive approaches like mobile EEG. While task-unrelated stimuli are commonly added to a workplace simulation to estimate event-related cognitive processes, using eyeblink activity poses an alternative as it is inherent to human behavior. This study aimed to investigate the eye blink event-related EEG activity of fourteen subjects while working in a power-plant operator simulation - actively operating (active condition) or observing (passive condition) a real-world steam engine. The changes in event-related potentials, event-related spectral perturbations, and functional connectivity under both conditions were analyzed. Our results indicated several cognitive changes in relation to task manipulation. Posterior N1 and P3 amplitudes revealed alterations associated with task complexity, with increased N1 and P3 amplitudes for the active condition, indicating greater cognitive effort than the passive condition. Increased frontal theta power and suppressed parietal alpha power were observed during the active condition reflecting high cognitive engagement. Additionally, higher theta connectivity was seen in fronto-parieto-centro-temporo-occipital regions as task demands increased, showing increased communication between brain regions. All of these results suggest using eye blink-related EEG activity to acquire a comprehensive understanding of neuro-cognitive processing while working in realistic environments.**

***Index Terms*— EEG, ERP, ERSP, neurophysiology, eye blink activity, functional connectivity, cognitive states.**

I. Introduction

IN RECENT decades, there have been several attempts to objectively evaluate cognitive states in work-related contexts to prevent hazardous situations resulting from either cognitive under- or overload [1]. The objective quantification of physical strain at workplaces has been mandatory for many decades, resulting in various thresholds for a worker's bearable physical load. Given the growing proportion of sedentary office work, there is a rising need for objective quantification of psychological strain using different measurement techniques (e.g., EEG, ECG, pupillometry) [2]. While subjective and behavioral measures give insights into such states, their temporal precision is rather restricted. In terms of temporally precise measuring techniques, the EEG has been identified as one of the most suitable methods to evaluate event-related cognitive processes – using event-related potentials (ERPs) – or over longer periods – using measures in the frequency domain.

Within work-related environments that are strongly reliant on visual information, e.g., a power-plant operator workplace, the detection of covert attentional processes is very important. This might be restricted using just overtly shown behavior. By using neurophysiological measures in realistic working environments – so-called *neuroergonomics* – there is an opportunity to overcome the inability to estimate covert cognitive changes [3]. Here, mobile EEG is a very useful tool due to its portability, long battery life, and high temporal resolution [4]. While the estimation of cognitive states in workplace simulations has been successful using EEG spectral measures over longer periods [5], [6], there has been no possibility to look into event-related attentional processes without adding external events to the task [7].

This restriction can be overcome by using events that are inherent to the human itself, namely eyeblink activity. In previous years it was shown that eye blinks are not a mere action to moisturize the eye or to prevent harmful environmental influences but to chunk the ongoing visual (and auditory) information intake. Therefore, blinking behavior is influenced by cognitive processes, as shown by [8] and [9], whose findings suggest that eye blinks become less frequent as cognitive demands rise, reflecting an inverse relationship between blink rate and task difficulty. Still, the analysis of related cognitive processes using the EEG is rather insightful. In the 1980s, an event-related potential was found after a blink in illuminated conditions – as opposed to blinking in a pitch-black room – comparable to one found after experimental visual stimulation [10]. In the following years, several studies also highlighted the importance of eye blinks for everyday information structuring to reflect cognitive processes [11] during visual [12] or auditory tasks [13]. While these studies showed that it was possible to deduct useful information from laboratory environments, blinks were shown to represent useful structuring events in real-life situations while walking either on a patch of lawn or in an inner city setting [14], [15].

Manuscript received 27 September 2022; revised 24 November 2022 and 23 January 2023; accepted 29 January 2023. Date of publication 3 February 2023; date of current version 8 February 2023. *(Corresponding author: Emad Alyan.)*

This work involved human subjects or animals in its research. Approval of all ethical and experimental procedures and protocols was granted by the local ethics committee of the Leibniz-Institut für Arbeitsforschung an der TU Dortmund.

Emad Alyan, Edmund Wascher, Stefan Arnau, and Julian Elias Reiser are with the Department of Ergonomics, Leibniz Research Centre for Working Environment and Human Factors, 44139 Dortmund, Germany (e-mail: alyan@ifado.de).

Ruth Kaesemann is with the Faculty of Mechanical Engineering, FH Dortmund, 44139 Dortmund, Germany.

Digital Object Identifier 10.1109/TNSRE.2023.3241962

When analyzing event-related cognitive processing, dozens of equal events are needed, necessitating the presentation of certain (visual) stimuli or – here – blinks that act as a visual stimulus. When light hits the retina after the eye-opening, a new ‘’stimulus” is presented that needs to be processed by sensory and attentional regions of the brain. By averaging over these equal events, the signal-to-noise ratio is increased, and spontaneous noise fluctuations will be (partially) eliminated [16].

Given the impact of blinks on brain-related and cognitive activity, recent literature [12], [14] contradicts arbitrarily categorizing blinks as artifacts. Interestingly, previous studies [17], [18] noticed a rise in low-frequency band (delta) signal time-locked to the blink at rest. Around the maximum of eye blinks, Bonfiglio et al. [19], [20] documented event-related synchronizations and de-synchronizations of the EEG, which were considered in the context of conscious processing information. They reported that blink-related delta oscillations could represent brain processes associated with self-consciousness and environmental awareness [19]. Unlike resting state studies, Liu et al. [21] demonstrated that blink-related activities are dynamically regulated to match internal cognitive processing demands in varied external settings during a task that requires repetitive reading. Additionally, they confirmed in another [22] that the areas of the ventral attention network are engaged during blink-related mental arithmetic tasks.

To evaluate whether an event-related approach is feasible for real-life cognitive state determination, a workplace simulation study consisting of a series of alternating active and passive power plant operator conditions was conducted. To retrieve blink event markers, a pattern-matching technique was used [14]. The active task consisted of actively adjusting the temperature of a miniature one-cylinder steam engine. In contrast, the passive task required the subject to vigilantly observe the system and note system temperatures following a visual signal in semi-random time intervals.

With the help of blink-related ERPs (bERPs), stimulus processing was investigated using well-studied components (P1, N1, N2, and P3). Early processing of stimuli is related to the P1 and N1 components, the first positive and negative deflection after the blink, which is responsive to the physical properties of the inputs [23]. These two components develop in the occipital cortex and are controlled by attention [24]. An increase in P1 and N1 amplitude indicates a higher amount of selective attention being needed for stimulus processing [25]. This assertion was further supported by Fu & Parasuraman. [26], claiming that the P1 component is a highly sensitive indicator of visuospatial attention allocation. This impact could also be observed in anterior N2, the second negative deflection after blinking, linked to executive functioning [27]. Allison and Polich [28] revealed that the amplitude of anterior N2 decreases in response to high-demanding tasks. Also, Kramer et al. [29] observed a decline in N2 amplitude as the difficulty of a radar monitoring task increased. The P3 component, the third positive deflection after the blink, can also be modulated by attention during different visuomotor task demands [30], [31], [32]. It corresponds adversely with task complexity [33] and is correlated with stimulus updating and attentional narrowing towards pertinent information [34]. The P3 amplitude was found to be higher when more attentional resources were devoted to the evoking stimuli [33], [34], [36].

Event-related spectral perturbation (ERSP) can also assist in identifying the impacts of task demands by measuring the power variations of a given frequency band in relation to a task-unrelated baseline [37]. Numerous studies suggest that EEG bands, particularly the theta and alpha bands, may be influential cognitive load predictors [38], [39], [40]. For instance, alpha activity between 8 and 12 Hz was found to be sensitive to mental workload levels [40], mental fatigue [41], [42], and occurrences of mind wandering [43]. It plays a vital role in conditions requiring a high level of visual-attentional processing [44]. Kamzanova et al. [45] showed that a rise in alpha activity could negatively correlate with attention. Alpha suppression, on the other hand, appears to be associated with task difficulty increases, possibly due to increased task involvement [46]. The most noticeable changes in alpha activity are mainly localized in occipital and parietal regions [5], [39]. Additionally, the change in theta power between 4 and 7 Hz positively correlates with spent cognitive resources [40], [47] and task complexity [48], [49]. Theta power appears to rise when sustained concentration is required during task execution [5], [49]. Here, frontal cortex areas are mainly linked with theta activity [5].

Besides ERPs and ERSPs, functional connectivity has been used to explore complex brain region connections to better understand the functional brain organization by capturing localized functions and communication among brain areas. According to the literature, this approach tends to assist in comprehending executive functioning by synchronizing cortical activity between functionally related brain areas [50], [51]. Involvement in cognitively demanding tasks, such as executive control, has been linked to increased functional connectivity [52]. Sciaraffa et al. [53] found that a more difficult task showed significantly higher interconnections in the theta band over the frontal brain area than in an easy task.

Several predictions are possible based on this working hypothesis. We expect increased posterior N1 and P3 amplitudes due to the active power plant operator settings, which should enhance attentional allocation because of increasing cognitive and visual demands. In contrast, the anterior N2 amplitude, which is a proven predictor of executive control and sensitivity to work demands, may decrease during the more demanding task (active condition). Additionally, active operator settings may tend to increase frontal theta power while decreasing alpha parietal power due to more task engagement. The active workload setting is anticipated to increase the strength of theta connectivity between the frontal (executive and planning) and other areas (sensory, motor, and cognitive) due to increased engagement of cognitive-motor processes.

II. Methods

A. Participants

For this study, 18 participants (16 male, 2 female) were recruited using online announcements in engineering classes of

Fig. 1. Miniature steam-engine. The water is filled into the tank and heated using a Bunsen burner. The ascending steam then flows through the copper steam tubes through the one-cylinder steam machine, finally reaching the condensation tube where the steam condenses and is transported out of the system. For the active condition, the gas supply can be manipulated to manage the resulting heat using a valve. Also, the steam that runs through the steam engine can be controlled via a steam valve. All pressure and temperature values can be accessed using a dial and an LED display (marked as X).

the FH Dortmund and mail newsletters of the FH Dortmund's student association for engineering studies. Data acquisition took place between February and December 2019. All participants had no prior or present neurologic or psychiatric condition, had a normal or corrected-to-normal vision, were free of hearing deficiencies, were right-handed, and had no motor or gait impairment. Four of these 18 participants had to be excluded from analysis due to faulty trigger markers in the EEG data, which rendered condition segmentation impossible. The age range of the remaining participants was between 22 and 35 years (M = 27.29, SD = 4.45). Subjects received compensation of 10€per hour and gave their informed written consent. The study was approved by the local ethics committee of the Leibniz Research Centre for Working Environment and Human Factors and was conducted in accordance with the Declaration of Helsinki.

B. Apparatus and Stimuli

The measurements took place in a seminar room equipped with a miniaturized steam machine with a single engine (see Fig. 1). To power the engine, water was boiled in the water tank until vaporizing and ascending into the steam engine. The amount of generated steam could be controlled by regulating the heat within the water tank using an adjustable Bunsen burner. Also, a valve between the water tank and the steam engine allowed for the manipulation of the steam passing through the engine at any given time. In the last step, the steam condensed after passing the engine, and condensed water was collected below the steam engine apparatus. This miniature steam engine, therefore, allowed the participants to regulate pressure levels in the water tank and the electricity generated by the engine (see Fig. 1). On top of the steam engine apparatus, a Raspberry Pi 2B (Raspberry Pi Foundation, Cambridge, UK) was placed to generate trigger signals recorded in the ongoing EEG data stream to allow for later segmentation of the data. The Raspberry pi was also extended with a blue diode to present visual stimuli to the participant. By changing USB thumb drives, the sequence of visual stimuli was determined.

The participants were assigned to two distinct tasks. Initially, they were required to operate the steam engine to reach a specific pressure level in the water tank. To do so, they had to regulate the heat supply, the quantity of incoming cooling water, and the pressure valve to attain the desired pressure level and maintain it for a short period to stabilize the system's state. Afterward, they recorded the temperature of the water tank, the temperature of the incoming cooling water, and the temperature of the outgoing cooling water. They then calculated the difference in temperature between the incoming and outgoing cooling water. The starting pressure was set at 0.8 bar, and the participants were instructed to increase it incrementally by 0.2 bar. In this active scenario, the blue diode of the Raspberry Pi served only to indicate the start (2 flashes) and end (3 flashes) of each block.

In the second task, participants did not actively manipulate the machine but passively observed the system and the Raspberry pi diode. Throughout the block, the diode lit up three times in quasi-random time intervals (with at least 2 minutes in between flashes), indicating that the participant had to mark down the water tank temperature. The flashes were only shown briefly (2s) to ensure that participants had to supervise the diode carefully. As in the first condition, the diode also indicated the beginning (2 flashes) and end (3 flashes) of a block. The order of conditions was the same for all subjects: they started with the active task followed by the passive task. This procedure was repeated two times, meaning that every participant completed three active and three passive tasks. Each condition block had a length of seven minutes, adding up to 42 minutes of experimentation time.

C. Procedure

Upon arrival in the morning at around 10 am, the participants were greeted by the experimenters and sat on a chair in the room to read the experiment's information sheet and sign the informed written consent form. Followingly, they were fitted with a 30-electrode cap and a drop-down ECG electrode (for more detailed information, see *D*).

D. Electrophysiological Data Acquisition

EEG data were acquired using 30 active electrodes (Brain Products GmbH, Gilching, GER) in a standard 10-20-system montage (Fp1, Fp2, F3, F4, F7, F8, Fz, FC1, FC2, FC5, FC6, C3, C4, Cz, T7, T8, CP1, CP2, CP5, CP6, P3, P4, P7, P8, Pz, PO9, PO10, O1, O2, Oz). The actively shielded electrodes were inserted into electrode holders after a tight flexible cap (actiCap, Brain Products GmbH, Gilching, GER). After the fitting process, the electrodes were filled with electrolyte gel until an impedance of 10 kΩ was reached. Special attention was paid to cable management so that electrode cables were carefully aligned to not cross each other or sway around while the participant was moving. FCz was used as an online reference, and AFz served as the ground. Every cable was routed through specific cable mounts of the actiCap next to the participant's ears. To further reduce cable motion, the

cables from the left and the right side were bundled using adhesive tape. The EEG cables were routed to the mobile amplifier (LiveAmp 32, Brain Products GmbH, Gilching, GER) placed at the back of the participant's head. The EEG data were recorded with a sampling frequency of 500 Hz and a bit depth of 24 bits. The recordings were stored offline on a micro SD card inserted into the LiveAmp 32 while the ongoing signal was observed using a Bluetooth connection to a Windows laptop running the BrainVision Recorder software (BrainProducts GmbH, Gilching, GER). Upon finishing the experiment, the data was transferred from the micro SD card to the laptop and converted into EEGLab readable files with the help of the LiveAmp File converter software (BrainProducts GmbH, Gilching, GER).

E. Data Processing

Data analyses were computed using MATLAB and EEGLAB custom scripts [54]. The raw EEG data were high-pass filtered at 0.1 Hz and low-pass filtered at 16 Hz using finite impulse response (FIR) filters (eegfiltnew) to remove environmental and muscular artifacts. Before re-referencing the data to the common average, the clean_artifacts function was used to search for and identify bad channels with default parameters (flatline = 0.5s, burst = 5, line noise = 4, correlation = 0.8, and window = 0.25). Next, the data were filtered through a high-pass zero-phase Hamming window FIR filter with a cutoff at 1.5Hz. Afterward, the data were decomposed into statistically independent components (ICs) utilizing AMICA [55]. The independent components were then copied onto the average referenced data (the data used before the high-pass filtering).

For blink detection, the local maxima were sought using the time course of the IC that had the highest correlation with the averaged anterior EEG activity [14]. A Gaussian curve was fitted in a temporal frame of +/− 120 ms around these local maxima. Valid blinks were those with a sufficient Gaussian waveform (goodness of fit, r-squared > 0.80) and an amplitude greater than 75% of the median amplitude of all peaks. The results showed that the active group had a blink rate of approximately 19.5±3.7 per minute, while the passive group had a blink rate of 19.8±5.7 per minute. The IClabel algorithm was then used to classify components automatically to finally remove any ICs that were not brain-related [56] (any components with $< 30\%$ brain and $> 30\%$ eye, muscle, heart, channel, and other classification probability). The average number of removed artifactual ICs per subject was 15.14 (standard deviation = 3.23). However, activity in the occipital region might be prone to overlapping visual and muscular components due to the free motion of subjects while performing the task. Thus, the cutoff frequency was set to 16 Hz and ICs with $> 30\%$ classed as muscle were excluded to eliminate most muscular artifacts.

The data was down-sampled to 250Hz, and epochs were extracted from −500 ms to 1200 ms relative to the eye blink maximum. Next, the acquired epochs were fed into an automatic epoch rejection EEGLAB function "pop_autorej" to exclude those with fluctuations exceeding an absolute threshold value of 500 μV and standard deviation threshold of 5 using an iterative approach (maximum rejection per iteration is 10%).

TABLE I
SEARCH WINDOWS AND PEAK LATENCIES (MS) OF THE ACTIVE AND PASSIVE CONDITION-RELATED BLINK MAXIMUM

Brain region	ERP	Search window (ms)	Peak amplitude latency (ms) Active	Passive
Frontal	P1	50-150	84	91
	P2	150-250	170	171
	N2	200-280	245	246
	SFN	300-500	274	259
Parietal	N1	40-100	71	60
	P3	300-500	361	347
Occipital	N1	40-100	84	72
	P3	300-500	370	336

F. Data Analysis

1) ERPs: For each subject, epochs were baselined at an interval ranging from -300 to -100 ms relative to the blink maximum and then averaged across each experimental block ranging from 0 to 1000 ms for the two conditions (active and passive). To rule out the possibility of fluctuations in baseline activity causing variations in ERP amplitude, we investigated of the effect of baseline correction on the mean of the pre-blink period (-300 to -100) in both active and passive conditions and across blocks 1, 2, and 3. The results showed that there were no significant differences observed across the conditions and blocks. The effect of conditions on amplitude was then investigated for P1, P2, N2, and sustained frontal negativity (SFN) at frontal (Fz, FC1, and FC2) sites. N1 and P3 amplitudes were investigated at parietal (CP1, Pz and CP2) and occipital (O1 and O2) sites. Mean amplitudes were calculated using all epochs after rejection. We extracted mean amplitudes using peak detection because it offers an unbiased measure of amplitude. Otherwise, the peak amplitude could be distorted by noise and thus be an overestimation [16]. Therefore, the maximum peak was estimated in time windows based on visual inspection to determine the mean amplitude within a 40-ms window around the condition-specific peak. Table I shows the determined peak latencies for the different ERP components, brain regions, and experimental conditions. For instance, a frontal P1 was parametrized at 84 ms for the active and 91 ms for the passive task.

2) Time−Frequency Power: Changes in EEG power over time were quantified by analyzing blink-related spectral perturbations (bERSP) using Morlet wavelet transformation [57]. The Morlet Wavelet transformation computes the similarity of the input signal to Gaussian-windowed complex sinusoidal over time [58]. The spectrum was calculated using a frequency range of 2–16 Hz, corresponding to 16 different frequencies. Wavelet cycles from 3 to 8 were utilized to emphasize temporal and frequency accuracy. The results were expressed as a decibel (dB) change from a common pre-stimulus baseline by averaging the power spectra of the pre-blink period data (-400 to -200 ms) for each subject over both conditions' trials. The difference in the average power over all electrodes was

TABLE II
ESTIMATED FIXED EFFECTS FROM LME OF ERPS AT FRONTAL, PARIETAL, AND OCCIPITAL REGIONS DURING ACTIVE AND PASSIVE WORKLOAD TASKS

Brain region	ERP	Predictor	β ± SE	df	*t*-value	*p*-value
Frontal	P1	(Intercept)	0.729±0.297	13	2.452	**0.029***
		Condition	0.592±0.179	65	3.318	**0.001****
		Block	-0.183±0.155	65	-1.184	0.241
		Interaction	0.094±0.309	65	0.305	0.761
	P2	(Intercept)	-0.422±0.333	13	-1.266	0.228
		Condition	0.849±0.206	65	4.118	< **0.001*****
		Block	-0.171±0.179	65	-0.955	0.343
		Interaction	0.035±0.357	65	0.098	0.922
	N2	(Intercept)	-1.836±0.393	13	-4.668	< **0.001*****
		Condition	1.108±0.258	65	4.297	< **0.001*****
		Block	-0.322±0.223	65	-1.440	0.155
		Interaction	0.022±0.447	65	0.050	0.961
	SFN	(Intercept)	-1.716±0.309	13	-5.548	< **0.001*****
		Condition	1.279±0.25	65	5.117	< **0.001*****
		Block	-0.307±0.216	65	-1.416	0.161
		Interaction	-0.019±0.433	65	-0.043	0.966
Parietal	N1	(Intercept)	0.522±0.208	13	2.504	**0.026***
		Condition	-0.423±0.175	65	-2.42	**0.018***
		Block	0.056±0.151	65	0.370	0.713
		Interaction	-0.220±0.303	65	-0.727	0.47
	P3	(Intercept)	2.162±0.328	13	6.581	< **0.001*****
		Condition	-0.268±0.232	65	-1.156	0.252
		Block	0.3714±0.201	65	1.848	0.069
		Interaction	-0.313±0.402	65	-0.778	0.44
Occipital	N1	(Intercept)	-1.076±0.444	13	-2.426	**0.031***
		Condition	-0.636±0.241	65	-2.634	**0.011***
		Block	0.170±0.209	65	0.815	0.418
		Interaction	-0.676±0.418	65	-1.616	0.111
	P3	(Intercept)	4.246±0.397	13	10.699	< **0.001*****
		Condition	-1.709±0.329	65	-5.187	< **0.001*****
		Block	0.228±0.285	65	0.799	0.427
		Interaction	-0.574±0.571	65	-1.005	0.318

Note. The successive polynomial (linear form) and simple (passive - active) contrast coding were used for trial and condition, respectively. The df denotes degrees of freedom, β is the estimates, and SE represents the standard error. $^{*}p < 0.05$, $^{**}p < 0.01$ and $^{***}p < 0.001$.

computed to identify the changes caused across temporal and spectral domains during the two conditions. Afterward, the power series for two frequency bands—theta (4–7 Hz) and alpha (8–13 Hz) —were calculated.

3) Functional Connectivity: The functional connectivity between different brain regions was also estimated by computing the wavelet phase lag index (PLI) across trials, reflecting the substantial temporal variation for each frequency band. The PLI aims to obtain phase synchronization estimates that are insensitive to volume conduction [59]. It measures the asymmetry of the phase difference distribution between two-time series, in this case, the signal of a pair of EEG electrodes:

$$\mathrm{PLI}(t,\omega) = \left| \frac{1}{N} \sum_{n=1}^{N} sgn\left(Im\left[e^{j(\phi 1(t,\omega) - \phi 2(t,\omega))} \right] \right) \right| \quad (1)$$

where ϕ_1 and ϕ_2 are the phase values of electrodes 1 and 2 at time t and frequency ω, N refers to the total number of trials. The Im is the imaginary part of phase difference, || denotes the absolute values, and the sign stands for the signum function (returns −1, 0, or +1). The PLI values range from zero to one, where a value of one indicates maximum coupling strength, and zero means no coupling strength.

4) Brain Network Analysis: Using graph theoretical approaches, which portray brain connections as nodes and edges, we could evaluate regional brain network variations. The fixed average degree is the most fundamental measure for describing the connectivity matrix [60]. It quantifies the number of connections that are above a predefined threshold value. We set the average degree threshold to 12. All edges with a degree of 12 or higher were preserved, while edges with a degree less than 12 were set to 0. More specifically, nodes in the subgraph with an average degree of 12 are connected to at least 41% of the entire network (29 nodes). This percentage was selected to ensure the least number of nodes were connected when averaging the cortical networks for each participant across frontal, central, temporal, parietal, and occipital.

Regional connectivity differences for active versus passive operator tasks were assessed as follows: PLI values for active versus passive operator tasks were compared for each frequency band at each time point from 0 to 1000 ms using a two-tailed paired t-test. Condition differences in regional connectivity were assumed to be statistically significant if the p-value was lower than 0.05. The global, inter-, and intra-regional networks of specific electrode connections that induced regional connectivity effects were visualized by plotting the strongest connections (PLI values averaged within the significant window). To observe cortical reproducibility and patterns, 15 cortical networks, including 5 local networks (connections within the frontal, for example) and 10 global networks (between regions), were constructed from the connectivity values of the 30 individual channels. For each network, a symmetric square matrix representing the maximum connection values between the two regions was generated and averaged. The obtained networks are distributed across frontal (channels F7, F3, Fz, F4, F8), central (channel FC5, FC6, FC1, FC2, C3, Cz, C4), temporal (channel CP5, CP6, T7, T8, P7, P8), parietal (channel CP1, CP2, P3, P4, Pz), and occipital sites (channel O1, Oz, O2).

G. Statistical Analysis

Statistical analyses were conducted using MATLAB (Mathworks, Inc., Natick, MA, USA) and jamovi ver. 2.2.5. For ERP and ERSP measures, we calculated linear mixed-effects (LME) models to examine the impacts of condition and block differences for different ERP components and frequency bands in brain regions. The variables included in the model were between-subject (subjects), within-subject variables (condition and blocks), and interactions of predictors. LME allows for modeling between-participant variations in a random factor term while investigating the effect of independent factors. The model specification was as follows:

$$\begin{aligned} \text{Amplitudes}|\text{Bands} \sim 1 + \text{Condition} + \text{Trial} \\ + \text{Condition:Trial} + (1|\text{Subject}) \end{aligned} \quad (2)$$

where amplitudes represent the ERP component amplitudes, and Bands denote theta and alpha frequency power in dB. The model was adapted with restricted maximum likelihood (REML), which results in less biased estimates of the random

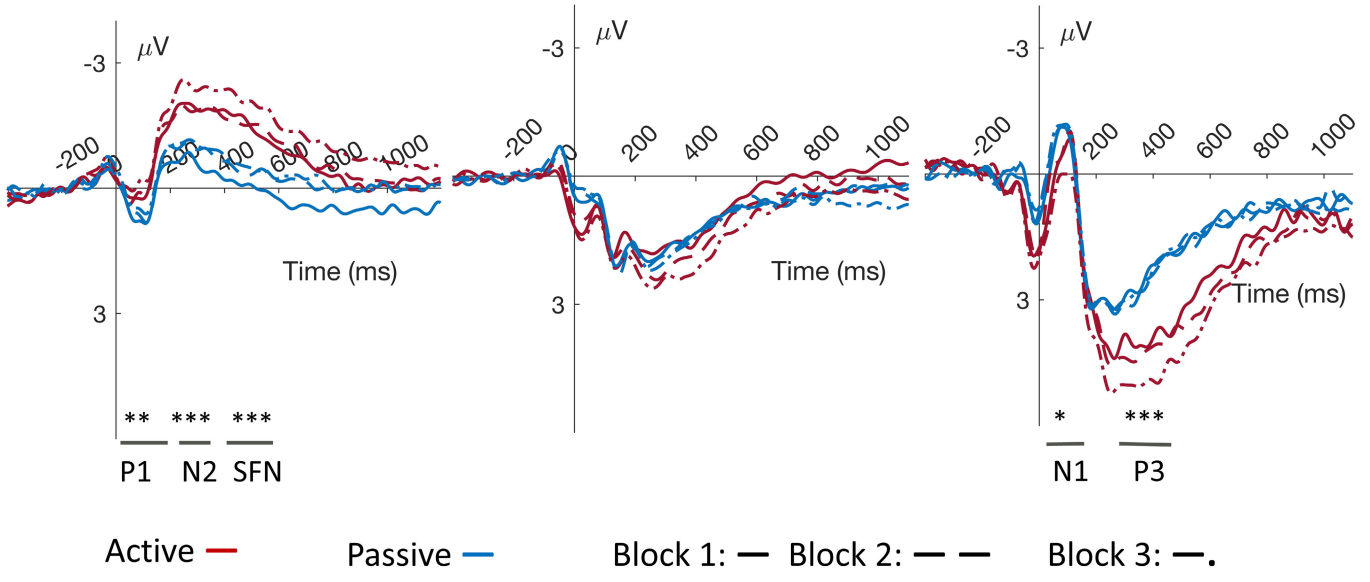

Fig. 2. Grand averaged event-related blink evoked potentials for the three blocks obtained at frontal (FC1, Fz, FC2), parietal (CP1, Pz, CP2), and occipital (O1, O2) sites. The ERP waves are shown for both active (red) and passive (blue) conditions. ERP peak amplitudes were calculated by performing peak detection on each epoch within a predetermined time window (frontal, P1: 50-150 ms, P2: 150-250 ms, N2: 200-280 ms, SFN: 300-500 ms; parietal/occipital, N1: 40-100 ms, P3: 300-500 ms). The data were then averaged within an interval of 40 ms window around the epoch-based peaks.

variance components. REML has been proposed for assessing fixed effects on small sample sizes [61]. The degrees of freedom were computed using the Satterthwaite approach [62] to produce p-values. For the connectivity analysis, the PLI data were transformed using the Fisher z-transformation (atanh, MATLAB function) to approximate the data to a normal distribution. Then, two-tailed paired t-tests with false discovery rate (FDR) correction [63] were calculated to compare connections across active and passive groups. The results were only deemed significant when the adjusted p-value was lower than the significance level of 0.05.

III. Results

A. ERPs

An LME was conducted on single-block mean amplitudes at the individual observation level to investigate ERP responses to conditions over the frontal, parietal and occipital regions (see Fig. 2 and 3). In the frontal region, the LME revealed significant main effects of operator task condition (active vs. passive) on frontal ERPs at P1(t (1, 65) = 3.318, p = 0.001), P2 (t (1, 65) = 4.118, p <.001), N2 (t (1, 65) = 4.297, p <.001) and SFN (t (1, 65) = 5.117, p <.001). There was no linear trend for the factor time, which was indicated by the insignificant differences in amplitudes of all ERPs across blocks, P1(t (2, 65) = −1.184, p = 0.241), P2 (t (2, 65) = −0.955, p = 0.343), N2 (t (2, 65) = −1.440, p = 0.155) and SFN (t (2, 65) = −1.416, p = 0.161). Also, the interaction of condition and block revealed no significant difference in frontal ERPs, P1(t (2, 65) = 0.305, p = 0.761), P2 (t (2, 65) = 0.098, p = 0.922), N2 (t (2, 65) = 0.050, p = 0.961) and SFN (t (2, 65) = −0.043, p = 0.966).

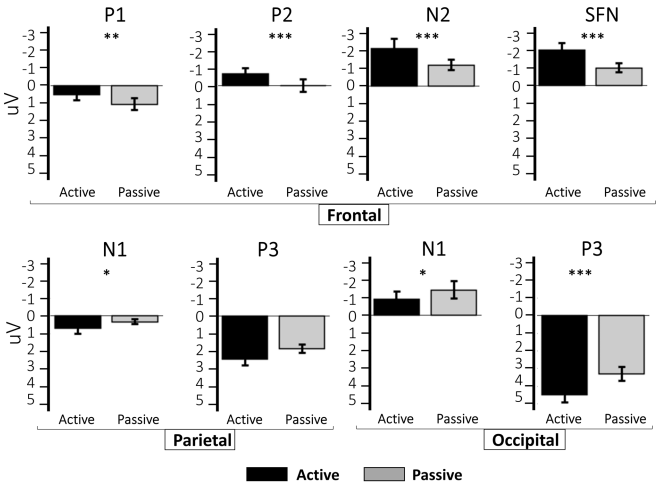

Fig. 3. The mean and standard deviation of blink-related EEG potential amplitudes at frontal (P1, P2, N2, and SFN), parietal (N1 and P3), and occipital sites (N1 and P3) during active and passive conditions. The amplitude of N1 and P3 in parietal and occipital areas increased during the active conditions. Frontal ERPs (P1, P2, N2, and SFN) exhibited an inverse effect.

Several substantial amplitude differences were also observable in parietal and occipital ERPs. The main effect of the condition was found to be significant for N1 amplitudes in parietal (t (1, 65) = −2.42, p = 0.018) and occipital areas (t (1, 65) = −2.634, p = 0.011). Additionally, P3 amplitude was significantly changed by operator task conditions occipital (t (1, 65) = −5.187, p <.001) but not parietal areas (t (1, 65) = −1.156, p = 0.252). The main factor block and its interaction with the condition were not statistically significant parietal (N1: block, t (2, 65) = 0.37, p = 0.713,

TABLE III

ESTIMATED FIXED EFFECTS FROM LME FOR THE ALPHA AND THETA FREQUENCY BANDS IN THE FRONTAL, CENTRAL, PARIETAL, AND OCCIPITAL AREAS DURING ACTIVE AND PASSIVE TASKS

EEG band	Latency	Predictor	L1: 0-200 ms				L2: 200-500 ms				L3: 500-1000 ms			
			β ± SE	df	*t*	*p*	β ± SE	df	*t*	*p*	β ± SE	df	*t*	*p*
Theta	Frontal	(Intercept)	0.386±0.239	13	1.616	0.13	-0.354±0.216	13	-1.639	0.125	-0.675±0.219	13	-3.082	**0.009****
		Condition	-0.732±0.193	65	-3.795	< **0.001*****	-0.577±0.168	65	-3.428	**0.001****	-0.338±0.155	65	-2.186	**0.032***
		Block	-0.098±0.167	65	-0.584	0.561	0.050±0.146	65	0.340	0.735	-0.030±0.134	65	-0.223	0.825
		Interaction	-0.056±0.334	65	-0.168	0.867	-0.262±0.292	65	-0.899	0.372	-0.014±0.268	65	-0.050	0.96
	Central	(Intercept)	0.361±0.239	13	1.510	0.155	-0.448±0.196	13	-2.283	**0.04***	-0.760±0.217	13	-3.503	**0.004****
		Condition	-1.015±0.229	65	-4.424	< **0.001*****	-0.709±0.206	65	-3.433	**0.001****	-0.392±0.178	65	-2.207	**0.031***
		Block	-0.027±0.199	65	-0.134	0.894	-0.078±0.179	65	-0.436	0.664	-0.024±0.154	65	-0.155	0.877
		Interaction	0.066±0.397	65	0.166	0.868	-0.018±0.357	65	-0.050	0.96	-0.054±0.308	65	-0.175	0.862
	Parietal	(Intercept)	0.417±0.209	13	1.995	0.067	-0.305±0.186	13	-1.638	0.125	-0.894±0.202	13	-4.420	< **0.001*****
		Condition	-1.125±0.261	65	-4.310	< **0.001*****	-0.959±0.243	65	-3.952	< **0.001*****	-0.367±0.210	65	-1.748	0.085
		Block	0.035±0.226	65	0.156	0.876	0.077±0.210	65	0.368	0.714	0.043±0.182	65	0.237	0.814
		Interaction	0.150±0.452	65	0.332	0.741	0.062±0.420	65	0.147	0.884	0.060±0.364	65	0.163	0.871
	Occipital	(Intercept)	1.029±0.218	13	4.720	< **0.001*****	0.058±0.157	13	0.366	0.718	-0.815±0.205	13	-3.968	**0.002****
		Condition	-1.457±0.182	65	-8.008	< **0.001*****	-1.656±0.188	65	-8.826	< **0.001*****	-1.001±0.173	65	-5.790	< **0.001*****
		Block	0.078±0.158	65	0.492	0.624	0.245±0.162	65	1.510	0.136	0.141±0.150	65	0.942	0.35
		Interaction	0.139±0.315	65	0.442	0.66	-0.019±0.325	65	-0.059	0.953	0.113±0.299	65	0.377	0.707
Alpha	Frontal	(Intercept)	0.315±0.123	78	2.569	**0.012***	-0.077±0.148	13	-0.517	0.614	-0.417±0.118	78	-3.521	< **0.001*****
		Condition	-0.069±0.245	78	-0.283	0.778	-0.022±0.255	65	-0.086	0.932	0.446±0.237	78	1.882	0.064
		Block	-0.037±0.212	78	-0.175	0.861	0.011±0.221	65	0.048	0.962	0.090±0.205	78	0.437	0.664
		Interaction	0.028±0.425	78	0.066	0.948	0.114±0.441	65	0.259	0.796	0.231±0.410	78	0.564	0.575
	Central	(Intercept)	0.427±0.149	13	2.872	**0.013***	-0.104±0.157	13	-0.662	0.519	-0.367±0.107	78	-3.429	< **0.001*****
		Condition	-0.210±0.232	65	-0.905	0.369	-0.238±0.236	65	-1.010	0.316	0.284±0.214	78	1.328	0.188
		Block	0.037±0.201	65	0.184	0.855	0.049±0.204	65	0.239	0.812	0.106±0.185	78	0.570	0.57
		Interaction	0.043±0.402	65	0.108	0.914	0.152±0.408	65	0.373	0.710	0.247±0.371	78	0.667	0.507
	Parietal	(Intercept)	0.673±0.157	13	4.293	< **0.001*****	-0.021±0.145	13	-0.146	0.886	-0.333±0.127	78	-2.630	**0.01***
		Condition	0.278±0.523	13	0.524	0.609	0.310±0.263	65	1.178	0.243	0.980±0.254	78	3.866	< **0.001*****
		Block	-0.053±0.084	52	-0.628	0.533	0.036±0.228	65	0.156	0.876	0.071±0.220	78	0.323	0.748
		Interaction	0.148±0.168	52	0.884	0.381	0.118±0.456	65	0.258	0.797	0.221±0.439	78	0.503	0.616
	Occipital	(Intercept)	0.620±0.153	13	4.060	**0.001****	0.064±0.177	13	0.361	0.724	-0.515±0.151	13	-3.403	**0.005****
		Condition	-1.908±0.208	65	-9.176	< **0.001*****	-1.846±0.250	65	-7.370	< **0.001*****	-1.169±0.242	65	-4.830	< **0.001*****
		Block	0.129±0.180	65	0.716	0.476	0.159±0.217	65	0.732	0.467	0.180±0.210	65	0.858	0.394
		Interaction	0.307±0.360	65	0.852	0.397	0.419±0.434	65	0.965	0.338	0.484±0.419	65	1.155	0.252

Note. The successive polynomial (linear form) and simple (passive - active) contrast coding were used for trial and condition, respectively. L represents the assigned interval. The df denotes degrees of freedom, β is the estimates, and SE represents the standard error. * $p < 0.05$, ** $p < 0.01$ and *** $p < 0.001$.

TABLE IV

STATISTICAL COMPARISON OF BRAIN CONNECTIVITY VALUES OF THE FIVE REGIONS UNDER ACTIVE AND PASSIVE WORKLOAD CONDITIONS

Brain connectivity	df	Active Mean	Active SD	Passive Mean	Passive SD	*t*-value	$p_{adj.}$
F	1(13)	0.087	0.065	0.087	0.053	0.034	0.974
FT	1(13)	0.165	0.064	0.137	0.039	2.503	**0.036***
FC	1(13)	0.137	0.034	0.117	0.022	2.852	**0.029***
FP	1(13)	0.159	0.055	0.13	0.049	2.944	**0.029***
FO	1(13)	0.17	0.055	0.129	0.058	2.264	**0.048***
T	1(13)	0.162	0.059	0.133	0.038	2.912	**0.029***
TC	1(13)	0.12	0.083	0.06	0.07	3.078	**0.029***
TP	1(13)	0.163	0.073	0.135	0.039	2.357	**0.043***
TO	1(13)	0.278	0.118	0.224	0.085	2.596	**0.036***
C	1(13)	0.128	0.039	0.114	0.029	1.938	0.08
CP	1(13)	0.158	0.059	0.127	0.035	2.521	**0.036***
CO	1(13)	0.174	0.068	0.143	0.04	2.885	**0.029***
P	1(13)	0.183	0.074	0.127	0.045	3.767	**0.018***
PO	1(13)	0.216	0.103	0.177	0.064	2.705	**0.034***
O	1(13)	0.236	0.1	0.141	0.071	4.137	**0.018***

Note. SD: standard deviation, p_{adj}: FDR-adjusted p-value, F: frontal, FT: frontal-temporal, FC: frontal-central, FP: frontal-parietal, FO: frontal-occipital, T: temporal, TC: temporal-central, TP: temporal-parietal, TO: temporal-occipital, C: central, CP: central-parietal, CO: central-occipital, P: parietal, PO: parietal-occipital, O: occipital.

interaction, t (2, 65) = −0.727, p = 0.47; P3: block, t (2, 65) = 1.848, p = 0.069, interaction, t (2, 65) = −0.778, p = 0.44) and occipital areas (N1: block, t (2, 65) = 0.815, p = 0.418, interaction, t (2, 65) = −1.616, p = 0.111; P3: block, t (2, 65) = 0.799, p = 0.427, interaction, t (2, 65) = −1.005, p = 0.318), reflecting that the amplitude of ERP components did not significantly change over time. All LME results are summarized in Table II.

B. ERSPs

The results of the LME on theta power showed that the main effect of the condition immediately after the blink maximum (L1: 0-200 ms) and at the L2 interval (200-500 ms) was significant at frontal (L1: t (1, 65) = −3.795, p <.001; L2: t (1, 65) = −3.428, p = 0.001), central (L1: t (1, 65) = −4.424, p <.001; L2: t (1, 65) = −3.433, p = 0.001), parietal (L1: t (1, 65) = −4.310, p <.001; L2: t (1, 65) = −3.952, p <.001), and occipital regions(L1: t (1, 65) = -8.008, p <.001; L2: t (1, 65) = -8.826, p <.001). In contrast to early intervals, the condition effect in theta power was less pronounced at the late interval (L3: 500–1000 ms), although a statistically significant effect was observed in frontal t (1, 65) = −2.186, p = 0.032), central t (1, 65) = −2.207, p = 0.031) and occipital areas (t (1, 65) = −5.790, p <.001).

Alpha power, on the other hand, demonstrated highly significant condition effects during the late interval (500-1000 ms) in the parietal region (t (1, 78) = 3.866,

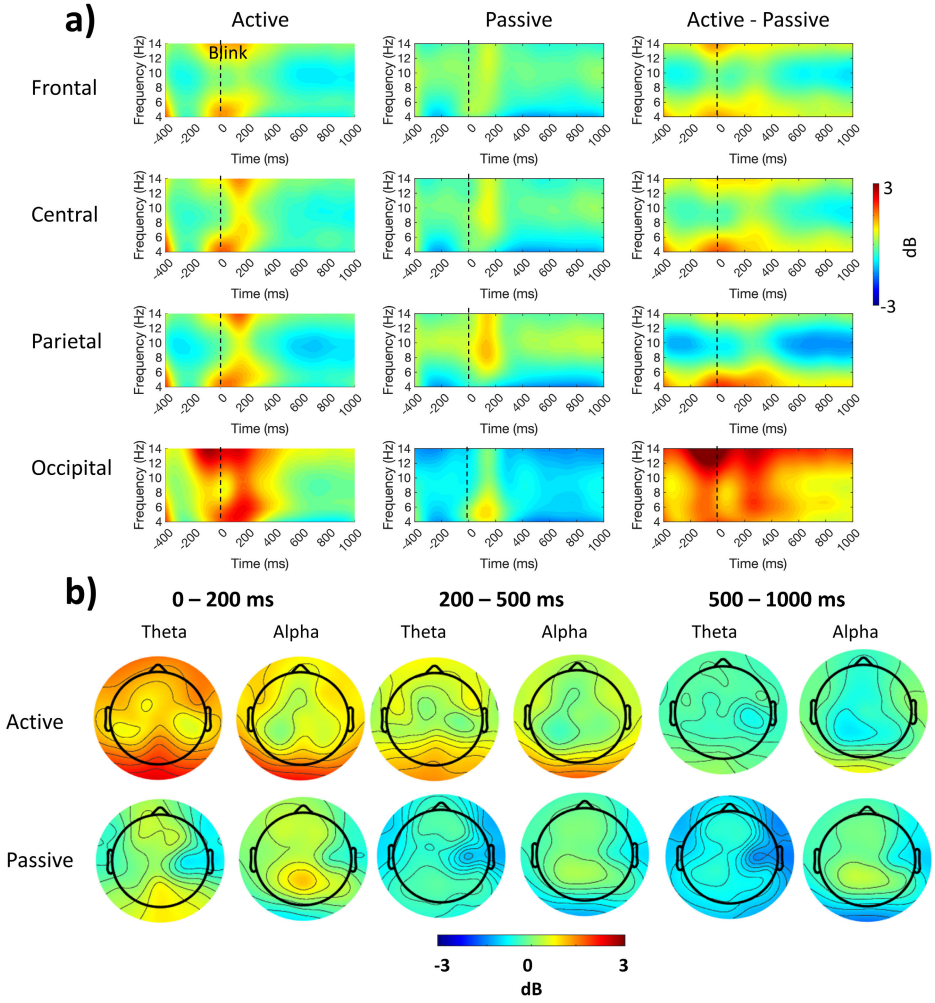

Fig. 4. a) ERSPs in response to blink-related activity during active and passive operator conditions. The ERSP plots are shown at frontal (FC1, Fz, FC2), central (Cz), parietal (CP1, Pz, CP2), and occipital sites (O1, O2) for EEG frequencies ranging from 4–14 Hz. b) Topography maps depict the changes in spectral power (in decibels) within the theta and alpha bands for the latency windows of 0-200ms, 200-500 ms, and 500-1000ms after the blink maximum.

p <.001), indicating elevated alpha during the passive task. No significant trends were observed for the main effect of condition in frontal (L1: t (1, 78) = −0.283, p = 0.778; L2: t (1, 65) = −0.086, p = 0.932; L3: t (1, 78) = 1.882, p = 0.064), and central sites (L1: t (1, 65) = −0.905, p = 0.369; L2: t (1, 65) = −1.010, p = 0.316; L3: t (1, 78) = 1.328, p = 0.188). Also, there were no effects of condition during the early intervals in parietal areas (L1: t (1, 13) = 0.524, p = 0.609; L2: t (1, 65) = 1.178, p = 0.243). Occipital alpha power showed a significant effect of condition in all intervals (L1: t (1, 65) = −9.176, p <.001; L2: t (1, 65) = −7.370, p <.001; L3: t (1, 65) = −4.830, p <.001). However, the main effect of the block and interaction effect did not reach significance in the theta or alpha frequency range in either model. The statistics of LME fixed effects for ERSPs are shown in Table III, while scalp maps and time-frequency plots are shown in Fig. 4.

C. Functional Connectivity

Fig. 5 shows the average PLI values of active and passive conditions across all electrodes during a time window starting at eyeblink maximum and ending 1000 ms after the onset for theta and alpha bands. Notable strong connections were reported between the onset and 400 ms (Fig. 5a). Three significant time windows of 100 ms were consecutively seen across the theta band (Fig. 5b) from 100-400 ms. However, connectivity values between conditions in the alpha range (8-13 Hz) remained insignificant ($p > 0.05$) at any given time window. Though the average degree threshold was set to 12, the global, inter-, and intra-networks were displayed with a threshold of 0.12 to better visualize the difference between conditions (see Fig. 6). After thresholding, the number of strong connections in all networks of the active condition group appeared to be high. Specifically, the changes in global connectivity networks mainly occurred in the left hemisphere, right frontocentral, and frontoparietal networks.

For the inter-hemispheric networks, the connectivity changes were primarily dominated in the left frontal-temporal to the right parietal-occipital networks, as well as within occipital networks and between parietal to temporal and left frontal to right parietal. For the intra-hemispheric networks, the changes were mainly located within the left

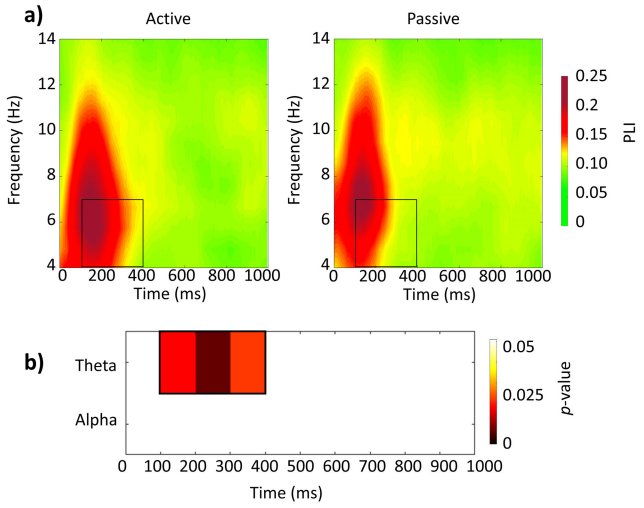

Fig. 5. Phase-lag index in active and passive operator task conditions. a) The time-frequency distribution maps of PLI are averaged for all electrodes. The horizontal axis shows the time (in milliseconds), which starts with zero (blink maximum) and ends at 1000 ms. The vertical axis reflects the frequency of the oscillations (Hz). b) The time series of averaged PLI values of all electrodes in the theta and alpha frequency band from zero ms (blink maximum) to 1000 ms. A two-tailed paired t-test was conducted to compare PLI values for active versus passive conditions within each 100 ms time window. Significant time windows ($p < 0.05$) are highlighted, reaching from black (highly significant) through red and yellow to white color (not significant). The results revealed significant PLI values within the theta band between 100-400 ms, while alpha did not reach significance at any time point.

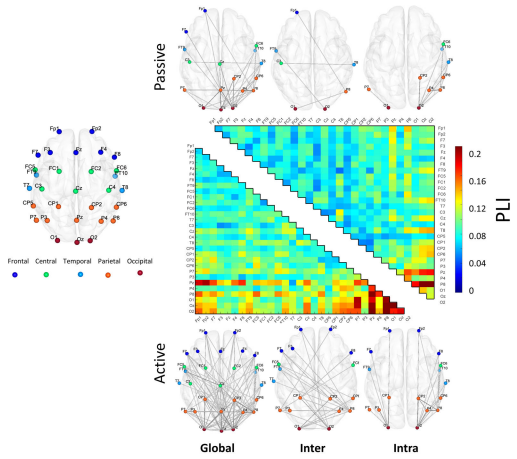

Fig. 6. Comparison of PLI values under active and passive conditions in the theta (100–400ms) band. The connectivity matrix shows strong connections between frontal leads and other leads over the scalp in the active group. The brain networks revealed significantly decreased connectivity (PLI values) in the passive group. The decreased connectivity was categorized into global, inter-, and intra-hemispheric networks. The dots represent measurement channels and are colored according to cortical location.

hemisphere networks and prefrontal to parietal in the right hemisphere.

The significance of the 15 networks derived from five primary brain areas of interest (frontal, central, temporal, parietal, and occipital) was then statistically evaluated using two-tailed paired t-tests with FDR correction. The results depicted in Fig. 7 and Table IV reveal that the connectivity

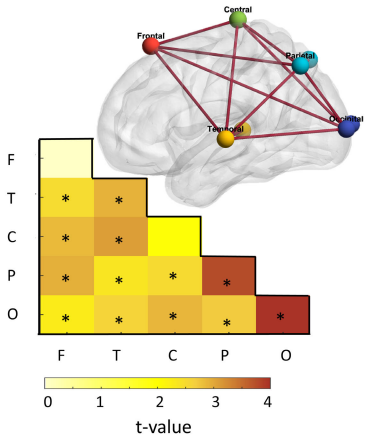

Fig. 7. Significantly increased connectivity in 13 networks of the active group. The dots represent cortical regions, and two neighboring dots of the same color denote connections within a cortical region. The heat map indicates the t-values of statistical difference between both conditions, color-coded from white (t = 0) through yellow to red (high).

of the active group was significantly higher ($p < 0.05$) in 13 networks. For instance, visual and attentional networks at occipital ($t(1,13) = 4.137$, $p = 0.018$) and parietal ($t(1,13) = 3.767$, $p = 0.018$) regions, respectively, exhibited a significant ($p < 0.05$) increased local connectivity in the active compared to the passive group. The difference was also found to be significant ($p < 0.05$) over temporal regions. Additionally, the increased operator activity (active task) demonstrated large-dispersed networks incorporating other significant regional connections ($p < 0.05$) such as frontal-occipital, frontal-parietal, frontal-central, frontal-temporal, occipital-temporal, occipital-parietal, occipital-central, parietal-central, parietal-temporal, and central-temporal. This may reflect an increase in cognitive control provided by the (frontally situated) central executive areas.

IV. Discussion

The investigation of operator state conditions poses a real challenge for ecologically valid neuroscientific studies when trying to gain a comprehensive understanding of cognitive states without introducing additional visual stimuli or secondary tasks. To overcome this drawback, we used eye blink activity (inherent to the subjects' behavior) to measure the participants' event-related EEG activity while operating (active condition) or observing (passive condition) a steam engine power plant simulation. The spontaneous but information-processing-related occurrences of blink events could be used to segment the continuous flow of visual information into time-locked activity [64]. Here, electrophysiological data were recorded using a mobile EEG device to demonstrate the influence of two operator task conditions on cognitive processes.

Different impacts were observed in several ERP components across cortical regions. For instance, the N1 amplitude in parietal and occipital areas was significantly affected by the operator state, indicating that the brain is more attuned to selective adjustment of visual demands induced by actively

operating the system. We also argue that the positivity for occipital and parietal electrodes at the eyeblink maximum could be related to the strength of brain oscillations resulting from visual processes that are still ongoing after the eyes close. Hohaia et al. [65] found that motion-sensitive visual processes can still take place even when the eyes are shut, which can lead to an increase in occipital alpha-band power. Despite the fact that there is other evidence that suggests neural activity following a blink is not necessarily of visual origin [66], the offset of visual stimuli during active and passive conditions created a potential for increased brain activity.

Additionally, the rise in the occipital P3 amplitude in active conditions most likely reflected resource allocation and updating processes due to being demanding. [67]. Moreover, frontal P1 and P2 appeared to be significantly decreased during the active condition. The P1 possibly indicated the increased involvement of filter functions of visual inputs during active conditions [68], [69], whereas the decreased P2 was related to higher-level perceptual processes [70], facilitating targeted information processing and identification relating to the manipulation of steam engine pressure. The frontal N2 and SFN also significantly decreased during active system manipulation, which may be attributed to attentional narrowing during processing complex information, leading to reduced information processing demands [71].

Furthermore, the high consistency of the bERP and bERSP responses was observed across condition blocks, indicating that mental fatigue did not develop over time. In support of that, complex tasks performed in natural environments were claimed to maintain people's motivation or engagement [14]. They found a high consistency of blink-evoked responses across ERPs and ERSPs experimental blocks of different cognitive efforts while standing, walking, and navigating an obstacle course in a natural situation. However, the main effects of the operator condition showed a significant increase in frontal theta power after blink-onset from 0-1000 ms in the active compared to the passive condition. Comparable to frontal regions, theta power was also significantly increased throughout the trial (0-1000ms) for central and occipital regions and in the interval 0-500 ms for the parietal regions during the active condition. This could indicate that attentional tasks necessitate a greater degree of cognitive control [64]; consequently, more effort was required to select pertinent information [72]. Additionally, the parietal site showed a regional decrease in alpha power in the active condition, most likely because of its function in action regulation. Recent research also reported an inverse correlation between increased task complexity levels and alpha power in posterior regions [44], which is consistent with our findings. They observed alpha reduction during the turning motion correlated with increased visual-attentional processing demand. Similarly, Wascher et al [14] revealed a decline in Alpha power as the demands of the walking task increased.

Besides that, functional connectivity measures seemed more sensitive to the change in operator task in the theta than the alpha band, indicating significantly increased connectivity over most brain regions between 100 ms to 400 ms after blink-onset. An increase in the inter- and intra-regional connectivity was observed in the active condition, supporting the assumption that cortical connectivity increases in response to high levels of complexity [73], [74]. According to the literature, a positive correlation was found between the task difficulty and the connectivity (EEG coherence) in all bands, including theta, between premotor and other regions such as execution, sensory, and motor during a cognitive-motor task [74]. Remarkably, the higher theta functional connectivity seen in all cortical regions may be linked to enhanced cognitive capabilities and heightened states of awareness due to better information exchange across brain areas when participants engaged in the active task [75], [76]. For instance, the notable coupling of the frontal to the central, temporal, and parietal regions highlights its crucial role in regulating the interaction of sensory and cognitive resources [77], [78]. Increased fronto-parietal theta connection considerably synchronizes sensorimotor inputs, while both regions are important for attentional control, indicating greater sensory processing required to handle response/action situations. This is also in line with a study by Popov et al. [79], who found a strong theta connection across the frontal and parietal regions when the working memory load increases. Reiser et al. [80] also demonstrated that higher cognitive load had greater Theta connectivity in the frontal and right parietal regions in response to switch trials regarding the used motor scheme compared to no-switch trials.

In conclusion, blink-related EEG activity provides valuable information regarding mental and visual processing during active versus passive working conditions. Different blink-related EEG measures such as ERPs, ERSPs, and functional connectivities demonstrate a strong sensitivity to changes in operator state, indicating that individuals allocate more attentional resources during active segments in a workplace simulation task. In support of that, the P3 component amplitudes revealed alterations relating to the narrowing of attention, while posterior N1 amplitudes adapted to visual demands. Similarly, ERSPs in the theta band showed functionally feasible activation patterns that corresponded to the demands of the two tasks. In contrast, parietal alpha power significantly decreased within the late time interval, reflecting increased task involvement in the case of active compared to passive conditions. Additionally, functional connectivity in the occipital, parietal, central, temporal, frontal, and associated networks was significantly stronger in the active state than in the passive state. These connectivity measures can shed light on the cognitive-motor processes underlying the level of cognitive demands required for various cognitive-motor tasks.

While our findings show significant differences between cognitive states, some limitations need to be mentioned. For once, the sample was limited to students of a specific study program who knew how to handle the steam machine in advance of the experiment. Therefore, all subjects had the same base knowledge about the system, but the number of participants was rather limited. Though we found high effect sizes, a larger sample would be needed in future investigations to increase the power of the study. Additionally, a further

improvement in the algorithm employed for blink-related EEG events is required to prevent variations in the blink-on- and offset of short and long blinks from introducing latency differences in the neural response after the blink. Furthermore, the conditions were not adequately controlled with regard to workload, motor output, and visual input, which could have had an impact on the results. Further research should be conducted to ensure that these factors are more closely matched. Additionally, this study does not provide sufficient evidence to draw a definitive conclusion regarding the neural activity; rather, it is an indication of the neural modulations associated with the two real-life conditions. Also, the EEG system we used was limited to 32 electrodes back then. Future studies looking into blink-related EEG activity should take advantage of the technical advances and use at least 64 electrode set-ups to improve ICA decomposition for better blink detection and distinction between blinks and saccades.

V. Conclusion

In this study, it was shown that an event-related analysis of a real-world task could be achieved using events that are inherent to human information processing, namely eyeblink activity. Our results suggest that eye blink-related EEG activity can provide a comprehensive understanding of neuro-cognitive processing while working in realistic environments. This study provides evidence that eye blink-related EEG activity can be used to measure cognitive effort and engagement in naturalistic tasks. Future studies should further investigate the potential of eye blink-related EEG activity to assess cognitive demands in more complex environments.

References

[1] S. Miyake, "Multivariate workload evaluation combining physiological and subjective measures," *Int. J. Psychophysiol.*, vol. 40, no. 3, pp. 233–238, Apr. 2001, doi: 10.1016/S0167-8760(00)00191-4.

[2] M. A. Hogervorst, A.-M. Brouwer, and J. B. F. van Erp, "Combining and comparing EEG, peripheral physiology and eye-related measures for the assessment of mental workload," *Frontiers Neurosci.*, vol. 8, p. 322, Oct. 2014. Accessed: Sep. 8, 2022. [Online]. Available: https://www.frontiersin.org/articles/10.3389/fnins.2014.00322

[3] E. Wascher et al., "Neuroergonomics on the go: An evaluation of the potential of mobile EEG for workplace assessment and design," *Hum. Factors*, vol. 65, no. 1, pp. 86–106, 2022, doi: 10.1177/00187208211007707.

[4] R. K. Mehta and R. Parasuraman, "Neuroergonomics: A review of applications to physical and cognitive work," *Frontiers Hum. Neurosci.*, vol. 7, p. 889, Dec. 2013, doi: 10.3389/fnhum.2013.00889.

[5] G. Borghini, L. Astolfi, G. Vecchiato, D. Mattia, and F. Babiloni, "Measuring neurophysiological signals in aircraft pilots and car drivers for the assessment of mental workload, fatigue and drowsiness," *Neurosci. Biobehav. Rev.*, vol. 44, pp. 58–75, Jul. 2014, doi: 10.1016/j.neubiorev.2012.10.003.

[6] E. Wascher et al., "Frontal theta activity reflects distinct aspects of mental fatigue," *Biol. Psychol.*, vol. 96, pp. 57–65, Feb. 2014, doi: 10.1016/j.biopsycho.2013.11.010.

[7] P. Mijović et al., "Towards continuous and real-time attention monitoring at work: Reaction time versus brain response," *Ergonomics*, vol. 60, no. 2, pp. 241–254, Feb. 2017, doi: 10.1080/00140139.2016.1142121.

[8] J. A. Veltman and A. W. K. Gaillard, "Physiological workload reactions to increasing levels of task difficulty," *Ergonomics*, vol. 41, no. 5, pp. 656–669, May 1998, doi: 10.1080/001401398186829.

[9] G. C. Drew, "Variations in reflex blink-rate during visual-motor tasks," *Quart. J. Exp. Psychol.*, vol. 3, no. 2, pp. 73–88, Apr. 1951, doi: 10.1080/17470215108416776.

[10] P. Berg and M. B. Davies, "Eyeblink-related potentials," *Electroencephalogr. Clin. Neurophysiol.*, vol. 69, no. 1, pp. 1–5, Jan. 1988, doi: 10.1016/0013-4694(88)90029-6.

[11] R. Goldstein, L. O. Bauer, and J. A. Stern, "Effect of task difficulty and interstimulus interval on blink parameters," *Int. J. Psychophysiol.*, vol. 13, no. 2, pp. 111–117, Sep. 1992, doi: 10.1016/0167-8760(92)90050-L.

[12] E. Wascher, H. Heppner, T. Möckel, S. O. Kobald, and S. Getzmann, "Eye-blinks in choice response tasks uncover hidden aspects of information processing," *EXCLI J.*, vol. 14, pp. 1207–1218, Nov. 2015, doi: 10.17179/excli2015-696.

[13] S. O. Kobald, E. Wascher, H. Heppner, and S. Getzmann, "Eye blinks are related to auditory information processing: Evidence from a complex speech perception task," *Psychol. Res.*, vol. 83, no. 6, pp. 1281–1291, Sep. 2019, doi: 10.1007/s00426-017-0952-9.

[14] E. Wascher, S. Arnau, M. Gutberlet, L. L. Chuang, G. Rinkenauer, and J. E. Reiser, "Visual demands of walking are reflected in eye-blink-evoked EEG-activity," *Appl. Sci.*, vol. 12, no. 13, p. 6614, Jun. 2022, doi: 10.3390/app12136614.

[15] A. Wunderlich and K. Gramann, "Eye movement-related brain potentials during assisted navigation in real-world environments," *Eur. J. Neurosci.*, vol. 54, no. 12, pp. 8336–8354, Dec. 2021, doi: 10.1111/ejn.15095.

[16] S. J. Luck, *An Introduction to the Event-Related Potential Technique*, 2nd ed. Cambridge, MA, USA: MIT Press, 2014.

[17] C. C. Liu, S. G. Hajra, T. P. L. Cheung, X. Song, and R. C. N. D'Arcy, "Spontaneous blinks activate the precuneus: Characterizing blink-related oscillations using magnetoencephalography," *Frontiers Hum. Neurosci.*, vol. 11, p. 489, Oct. 2017. Accessed: Nov. 21, 2022. [Online]. Available: https://www.frontiersin.org/articles/10.3389/fnhum.2017.00489

[18] L. Bonfiglio, S. Sello, P. Andre, M. C. Carboncini, P. Arrighi, and B. Rossi, "Blink-related delta oscillations in the resting-state EEG: A wavelet analysis," *Neurosci. Lett.*, vol. 449, no. 1, pp. 57–60, Jan. 2009, doi: 10.1016/j.neulet.2008.10.039.

[19] L. Bonfiglio et al., "Cortical source of blink-related delta oscillations and their correlation with levels of consciousness," *Hum. Brain Mapping*, vol. 34, no. 9, pp. 2178–2189, Sep. 2013, doi: 10.1002/hbm.22056.

[20] L. Bonfiglio, S. Sello, M. C. Carboncini, P. Arrighi, P. Andre, and B. Rossi, "Reciprocal dynamics of EEG alpha and delta oscillations during spontaneous blinking at rest: A survey on a default mode-based visuo-spatial awareness," *Int. J. Psychophysiol.*, vol. 80, no. 1, pp. 44–53, Apr. 2011, doi: 10.1016/j.ijpsycho.2011.01.002.

[21] C. C. Liu, S. G. Hajra, G. Pawlowski, S. D. Fickling, X. Song, and R. C. N. D'Arcy, "Differential neural processing of spontaneous blinking under visual and auditory sensory environments: An EEG investigation of blink-related oscillations," *NeuroImage*, vol. 218, Sep. 2020, Art. no. 116879, doi: 10.1016/j.neuroimage.2020.116879.

[22] C. C. Liu, S. G. Hajra, X. Song, S. M. Doesburg, T. P. L. Cheung, and R. C. N. D'Arcy, "Cognitive loading via mental arithmetic modulates effects of blink-related oscillations on precuneus and ventral attention network regions," *Hum. Brain Mapping*, vol. 40, no. 2, pp. 377–393, Feb. 2019, doi: 10.1002/hbm.24378.

[23] H. M. Morgan, C. Klein, S. G. Boehm, K. L. Shapiro, and D. E. J. Linden, "Working memory load for faces modulates P300, N170, and N250r," *J. Cogn. Neurosci.*, vol. 20, no. 6, pp. 989–1002, Jun. 2008, doi: 10.1162/jocn.2008.20072.

[24] C. S. Herrmann and R. T. Knight, "Mechanisms of human attention: Event-related potentials and oscillations," *Neurosci. Biobehav. Rev.*, vol. 25, no. 6, pp. 465–476, Aug. 2001, doi: 10.1016/S0149-7634(01)00027-6.

[25] B. D. Bartholow and D. M. Amodio, "Using event-related brain potentials in social psychological research: A brief review and tutorial," in *Methods in Social Neuroscience*. New York, NY, USA: Guilford Press, 2009, pp. 198–232.

[26] S. Fu and R. Parasuraman, "Event-related potentials (ERPs) in neuroergonomics," in *Neuroergonomics: The Brain at Work*, R. Parasuraman and M. Rizzo, Eds. London, U.K.: Oxford Univ. Press, 2006, doi: 10.1093/acprof:oso/9780195177619.003.0003.

[27] J. R. Folstein and C. Van Petten, "Influence of cognitive control and mismatch on the N2 component of the ERP: A review," *Psychophysiology*, vol. 45, no. 1, pp. 152–170, 2008, doi: 10.1111/j.1469-8986.2007.00602.x.

[28] B. Z. Allison and J. Polich, "Workload assessment of computer gaming using a single-stimulus event-related potential paradigm," *Biol. Psychol.*, vol. 77, no. 3, pp. 277–283, Mar. 2008, doi: 10.1016/j.biopsycho.2007.10.014.

[29] A. F. Kramer, L. J. Trejo, and D. Humphrey, "Assessment of mental workload with task-irrelevant auditory probes," *Biol. Psychol.*, vol. 40, no. 1, pp. 83–100, May 1995, doi: 10.1016/0301-0511(95)05108-2.

[30] F. B. Dyke et al., "The efficacy of auditory probes in indexing cognitive workload is dependent on stimulus complexity," *Int. J. Psychophysiol.*, vol. 95, no. 1, pp. 56–62, Jan. 2015, doi: 10.1016/j.ijpsycho.2014.12.008.

[31] M. W. Miller, J. C. Rietschel, C. G. McDonald, and B. D. Hatfield, "A novel approach to the physiological measurement of mental workload," *Int. J. Psychophysiol.*, vol. 80, no. 1, pp. 75–78, Apr. 2011, doi: 10.1016/j.ijpsycho.2011.02.003.

[32] J. C. Rietschel et al., "Psychophysiological support of increasing attentional reserve during the development of a motor skill," *Biol. Psychol.*, vol. 103, pp. 349–356, Dec. 2014, doi: 10.1016/j.biopsycho.2014.10.008.

[33] A. Kok, "On the utility of P3 amplitude as a measure of processing capacity," *Psychophysiology*, vol. 38, no. 3, pp. 557–577, May 2001, doi: 10.1017/S0048577201990559.

[34] J. Polich, "Updating P300: An integrative theory of P3a and P3b," *Clin. Neurophysiol.*, vol. 118, pp. 2128–2148, Oct. 2007, doi: 10.1016/j.clinph.2007.04.019.

[35] A. Kok, "Event-related-potential (ERP) reflections of mental resources: A review and synthesis," *Biol. Psychol.*, vol. 45, nos. 1–3, pp. 19–56, Mar. 1997, doi: 10.1016/S0301-0511(96)05221-0.

[36] R. Kuribayashi and H. Nittono, "High-resolution audio with inaudible high-frequency components induces a relaxed attentional state without conscious awareness," *Frontiers Psychol.*, vol. 8, p. 93, Feb. 2017. Accessed: Sep. 1, 2022. [Online]. Available: https://www.frontiersin.org/articles/10.3389/fpsyg.2017.00093

[37] W. Klimesch, "EEG alpha and theta oscillations reflect cognitive and memory performance: A review and analysis," *Brain Res. Rev.*, vol. 29, nos. 2–3, pp. 169–195, Apr. 1999, doi: 10.1016/S0165-0173(98)00056-3.

[38] A. Gevins et al., "Towards measurement of brain function in operational environments," *Biol. Psychol.*, vol. 40, no. 1, pp. 169–186, May 1995, doi: 10.1016/0301-0511(95)05105-8.

[39] S. Puma, N. Matton, P.-V. Paubel, É. Raufaste, and R. El-Yagoubi, "Using theta and alpha band power to assess cognitive workload in multitasking environments," *Int. J. Psychophysiol.*, vol. 123, pp. 111–120, Jan. 2018, doi: 10.1016/j.ijpsycho.2017.10.004.

[40] J. Xie, G. Xu, J. Wang, M. Li, C. Han, and Y. Jia, "Effects of mental load and fatigue on steady-state evoked potential based brain computer interface tasks: A comparison of periodic flickering and motion-reversal based visual attention," *PLoS ONE*, vol. 11, no. 9, Sep. 2016, Art. no. e0163426, doi: 10.1371/journal.pone.0163426.

[41] E. Wascher, H. Heppner, S. O. Kobald, S. Arnau, S. Getzmann, and T. Möckel, "Age-sensitive effects of enduring work with alternating cognitive and physical Load. A study applying mobile EEG in a real life working scenario," *Frontiers Hum. Neurosci.*, vol. 9, p. 711, Jan. 2016. Accessed: Sep. 12, 2022. [Online]. Available: https://www.frontiersin.org/articles/10.3389/fnhum.2015.00711

[42] S. Arnau, T. Brümmer, N. Liegel, and E. Wascher, "Inverse effects of time-on-task in task-related and task-unrelated theta activity," *Psychophysiology*, vol. 58, no. 6, Jun. 2021, Art. no. e13805, doi: 10.1111/psyp.13805.

[43] S. Arnau, C. Löffler, J. Rummel, D. Hagemann, E. Wascher, and A. Schubert, "Inter-trial alpha power indicates mind wandering," *Psychophysiology*, vol. 57, no. 6, Jun. 2020, Art. no. e13581, doi: 10.1111/psyp.13581.

[44] B. V. Ehinger et al., "Kinesthetic and vestibular information modulate alpha activity during spatial navigation: A mobile EEG study," *Frontiers Hum. Neurosci.*, vol. 8, p. 71, Feb. 2014. Accessed: Aug. 22, 2022. [Online]. Available: https://www.frontiersin.org/articles/10.3389/fnhum.2014.00071

[45] A. T. Kamzanova, A. M. Kustubayeva, and G. Matthews, "Use of EEG workload indices for diagnostic monitoring of vigilance decrement," *Hum. Factors*, vol. 56, no. 6, pp. 1136–1149, Sep. 2014, doi: 10.1177/0018720814526617.

[46] W. Klimesch, "Alpha-band oscillations, attention, and controlled access to stored information," *Trends Cogn. Sci.*, vol. 16, no. 12, pp. 606–617, Dec. 2012, doi: 10.1016/j.tics.2012.10.007.

[47] P. S. Tsang and M. A. Vidulich, "Mental workload and situation awareness," in *Handbook of Human Factors and Ergonomics*, 3rd ed. Hoboken, NJ, USA: Wiley, 2006, pp. 243–268, doi: 10.1002/0470048204.ch9.

[48] P. Antonenko, F. Paas, R. Grabner, and T. van Gog, "Using electroencephalography to measure cognitive load," *Educ. Psychol. Rev.*, vol. 22, no. 4, pp. 425–438, Dec. 2010, doi: 10.1007/s10648-010-9130-y.

[49] I. Käthner, S. C. Wriessnegger, G. R. Müller-Putz, A. Kübler, and S. Halder, "Effects of mental workload and fatigue on the P300, alpha and theta band power during operation of an ERP (P300) brain–computer interface," *Biol. Psychol.*, vol. 102, pp. 118–129, Oct. 2014, doi: 10.1016/j.biopsycho.2014.07.014.

[50] H. Mizuhara and Y. Yamaguchi, "Human cortical circuits for central executive function emerge by theta phase synchronization," *NeuroImage*, vol. 36, no. 1, pp. 232–244, May 2007, doi: 10.1016/j.neuroimage.2007.02.026.

[51] N. Zink, A. Lenartowicz, and S. Markett, "A new era for executive function research: On the transition from centralized to distributed executive functioning," *Neurosci. Biobehav. Rev.*, vol. 124, pp. 235–244, May 2021, doi: 10.1016/j.neubiorev.2021.02.011.

[52] P. Sauseng, J. Hoppe, W. Klimesch, C. Gerloff, and F. C. Hummel, "Dissociation of sustained attention from central executive functions: Local activity and interregional connectivity in the theta range," *Eur. J. Neurosci.*, vol. 25, no. 2, pp. 587–593, Jan. 2007, doi: 10.1111/j.1460-9568.2006.05286.x.

[53] N. Sciaraffa et al., "Brain interaction during cooperation: Evaluating local properties of multiple-brain network," *Brain Sci.*, vol. 7, no. 12, p. 90, Jul. 2017, doi: 10.3390/brainsci7070090.

[54] A. Delorme and S. Makeig, "EEGLAB: An open source toolbox for analysis of single-trial EEG dynamics including independent component analysis," *J. Neurosci. Methods*, vol. 134, no. 1, pp. 9–21, Mar. 2004.

[55] J. A. Palmer, K. Kreutz-Delgado, and S. Makeig, "AMICA: An adaptive mixture of independent component analyzers with shared components," Swartz Center Comput. Neursosci., Univ. California, San Diego, CA, USA, Tech. Rep., 2012.

[56] L. Pion-Tonachini, K. Kreutz-Delgado, and S. Makeig, "ICLabel: An automated electroencephalographic independent component classifier, dataset, and website," *NeuroImage*, vol. 198, pp. 181–197, Sep. 2019.

[57] M. X. Cohen, *Analyzing Neural Time Series Data: Theory and Practice*. Cambridge, MA, USA: MIT Press, 2014.

[58] A. Grinsted, J. C. Moore, and S. Jevrejeva, "Application of the cross wavelet transform and wavelet coherence to geophysical time series," *Nonlinear Processes Geophys.*, vol. 11, nos. 5–6, pp. 561–566, 2004, doi: 10.5194/npg-11-561-2004.

[59] C.J. Stam, G. Nolte, and A. Daffertshofer, "Phase lag index: Assessment of functional connectivity from multi channel EEG and MEG with diminished bias from common sources," *Hum. Brain Mapping.*, vol. 28, no. 11, pp. 1178–1193, Nov. 2007.

[60] M. Rubinov and O. Sporns, "Complex network measures of brain connectivity: Uses and interpretations," *NeuroImage*, vol. 52, no. 3, pp. 1059–1069, Sep. 2010, doi: 10.1016/j.neuroimage.2009.10.003.

[61] T. A. B. Snijders and R. J. Bosker, *Multilevel Analysis: An Introduction to Basic and Advanced Multilevel Modeling*. Newbury Park, CA, USA: Sage, 2011.

[62] F. E. Satterthwaite, "An approximate distribution of estimates of variance components," *Biometrics Bull.*, vol. 2, no. 6, pp. 110–114, Dec. 1946, doi: 10.2307/3002019.

[63] Y. Benjamini and Y. Hochberg, "Controlling the false discovery rate: A practical and powerful approach to multiple testing," *J. Roy. Stat. Soc. B, Methodol.*, vol. 57, no. 1, pp. 289–300, 1995, doi: 10.1111/j.2517-6161.1995.tb02031.x.

[64] E. Wascher, H. Heppner, and S. Hoffmann, "Towards the measurement of event-related EEG activity in real-life working environments," *Int. J. Psychophysiol.*, vol. 91, no. 1, pp. 3–9, Jan. 2014, doi: 10.1016/j.ijpsycho.2013.10.006.

[65] W. Hohaia, B. W. Saurels, A. Johnston, K. Yarrow, and D. H. Arnold, "Occipital alpha-band brain waves when the eyes are closed are shaped by ongoing visual processes," *Sci. Rep.*, vol. 12, no. 1, p.1194, Jan. 2022, doi: 10.1038/s41598-022-05289-6.

[66] D. Bristow, J.-D. Haynes, R. Sylvester, C. D. Frith, and G. Rees, "Blinking suppresses the neural response to unchanging retinal stimulation," *Current Biol.*, vol. 15, no. 14, pp. 1296–1300, Jul. 2005, doi: 10.1016/j.cub.2005.06.025.

[67] A. Miyake, N. P. Friedman, M. J. Emerson, A. H. Witzki, A. Howerter, and T. D. Wager, "The unity and diversity of executive functions and their contributions to complex 'frontal lobe' tasks: A latent variable analysis," *Cogn. Psychol.*, vol. 41, no. 1, pp. 49–100, Aug. 2000, doi: 10.1006/cogp.1999.0734.

[68] R. Lebib, D. Papo, S. de Bode, and P.-M. Baudonnière, "Evidence of a visual-to-auditory cross-modal sensory gating phenomenon as reflected by the human P50 event-related brain potential modulation," *Neurosci. Lett.*, vol. 341, no. 3, pp. 185–188, May 2003, doi: 10.1016/S0304-3940(03)00131-9.

[69] M. Lijffijt et al., "P50, N100, and P200 sensory gating: Relationships with behavioral inhibition, attention, and working memory," *Psychophysiology*, vol. 46, no. 5, pp. 1059–1068, Sep. 2009, doi: 10.1111/j.1469-8986.2009.00845.x.

[70] K. E. Crowley and I. M. Colrain, "A review of the evidence for P2 being an independent component process: Age, sleep and modality," *Clin. Neurophysiol.*, vol. 115, no. 4, pp. 732–744, Apr. 2004, doi: 10.1016/j.clinph.2003.11.021.

[71] L. M. Bonacci, S. Bressler, J. A. C. Kwasa, A. L. Noyce, and B. G. Shinn-Cunningham, "Effects of visual scene complexity on neural signatures of spatial attention," *Frontiers Hum. Neurosci.*, vol. 14, p. 91, Mar. 2020. Accessed: Aug. 22, 2022. [Online]. Available: https://www.frontiersin.org/articles/10.3389/fnhum.2020.00091

[72] J. E. M. Scanlon, E. X. Redman, J. W. P. Kuziek, and K. E. Mathewson, "A ride in the park: Cycling in different outdoor environments modulates the auditory evoked potentials," *Int. J. Psychophysiol.*, vol. 151, pp. 59–69, May 2020, doi: 10.1016/j.ijpsycho.2020.02.016.

[73] R. J. Gentili, T. J. Bradberry, H. Oh, B. D. Hatfield, and J. L. C. Vidal, "Cerebral cortical dynamics during visuomotor transformation: Adaptation to a cognitive-motor executive challenge," *Psychophysiology*, vol. 48, no. 6, pp. 813–824, Jun. 2011, doi: 10.1111/j.1469-8986.2010.01143.x.

[74] J. C. Rietschel, M. W. Miller, R. J. Gentili, R. N. Goodman, C. G. McDonald, and B. D. Hatfield, "Cerebral-cortical networking and activation increase as a function of cognitive-motor task difficulty," *Biol. Psychol.*, vol. 90, no. 2, pp. 127–133, May 2012, doi: 10.1016/j.biopsycho.2012.02.022.

[75] I. Kakkos et al., "Mental workload drives different reorganizations of functional cortical connectivity between 2D and 3D simulated flight experiments," *IEEE Trans. Neural Syst. Rehabil. Eng.*, vol. 27, no. 9, pp. 1704–1713, Sep. 2019, doi: 10.1109/TNSRE.2019.2930082.

[76] F. Taya, Y. Sun, F. Babiloni, N. V. Thakor, and A. Bezerianos, "Topological changes in the brain network induced by the training on a piloting task: An EEG-based functional connectome approach," *IEEE Trans. Neural Syst. Rehabil. Eng.*, vol. 26, no. 2, pp. 263–271, Feb. 2018, doi: 10.1109/TNSRE.2016.2581809.

[77] J. F. Cavanagh and M. J. Frank, "Frontal theta as a mechanism for cognitive control," *Trends Cogn. Sci.*, vol. 18, no. 8, pp. 414–421, Aug. 2014, doi: 10.1016/j.tics.2014.04.012.

[78] M. S. Clayton, N. Yeung, and R. Cohen Kadosh, "The roles of cortical oscillations in sustained attention," *Trends Cogn. Sci.*, vol. 19, no. 4, pp. 188–195, Apr. 2015, doi: 10.1016/j.tics.2015.02.004.

[79] T. Popov, P. Popova, M. Harkotte, B. Awiszus, B. Rockstroh, and G. A. Miller, "Cross-frequency interactions between frontal theta and posterior alpha control mechanisms foster working memory," *NeuroImage*, vol. 181, pp. 728–733, Nov. 2018, doi: 10.1016/j.neuroimage.2018.07.067.

[80] J. E. Reiser, E. Wascher, G. Rinkenauer, and S. Arnau, "Cognitive-motor interference in the wild: Assessing the effects of movement complexity on task switching using mobile EEG," *Eur. J. Neurosci.*, vol. 54, no. 12, pp. 8175–8195, Dec. 2021, doi: 10.1111/ejn.14959.